applied sciences

MDPI

Article

Kinematic Response of End-Bearing Piles under the Excitation of Vertical P-Waves Considering the Construction Effect

Denghui Dai [1,*], Yanjie Zhang [2], Yunfei Zhang [1], Zhanbin Wang [3] and Zhenya Li [1]

1 Key Laboratory of Ministry of Education for Geomechanics and Embankment Engineering, Hohai University, Nanjing 210024, China; 1804010411@hhu.edu.cn (Y.Z.); jllizhenya@hhu.edu.cn (Z.L.)
2 Yunnan Dianzhong Water Diversion Engineering Co., Ltd., Kunming 650000, China; yanjie_tm@163.com
3 College of Civil Engineering and Architecture, Nanjing Vocational Institute of Transport Technology, Nanjing 211188, China; wangzhanbin@njitt.edu.cn
* Correspondence: denghuidai@hhu.edu.cn

Abstract: Under most engineering conditions, soil disturbance due to pile installation may cause soil properties to vary within the region adjacent to the pile in the radial direction. This paper derives a rigorous solution to investigate the kinematic response of end-bearing piles under the excitation of vertical P-waves considering the construction effect. The displacement responses of piles and soil, governed by the dynamic equilibrium equation, are theoretically derived with the separation of variables method. The scattered waves induced by the pile–soil system, which is the key factor of the problem, are decoupled from the total wavefields. Moreover, the friction occurring at the interface of the soil and pile shaft are directly obtained. Thus, the present solution can accurately account for the pile–soil interaction. Comparisons between the numerical results of the present method and the available results are performed. A detailed discussion on the kinematic response coefficient, amplification factor, and soil motion is provided.

Keywords: soil–pile interaction; kinematic response; vertical P-wave; construction effect; analytical solution

check for updates

Citation: Dai, D.; Zhang, Y.; Zhang, Y.; Wang, Z.; Li, Z. Kinematic Response of End-Bearing Piles under the Excitation of Vertical P-Waves Considering the Construction Effect. *Appl. Sci.* **2022**, *12*, 3468. https://doi.org/10.3390/app12073468

Academic Editors: Yongxin Wu, Mi Zhao and Rui Wang

Received: 17 February 2022
Accepted: 28 March 2022
Published: 29 March 2022

1. Introduction

Piles are widely used as the foundations of infrastructures. The seismic response of piles plays an important role in the aseismic design of superstructures [1–8]. The investigation of the pile–soil dynamic interaction in the absence of a superstructure under a seismic wave incidence, known as a kinematic interaction, has been the focus of numerous studies [9–12].

Various theoretical approaches have been developed to investigate the lateral kinematic interaction of the pile–soil system. However, less attention has been paid to the vertical kinematic interaction. The vertical seismic motion at the pile head is often assumed as the free-field soil motion in the practical design of the pile–soil system. In fact, the scattering of seismic waves induced by the pile foundation will significantly modify the seismic response, which allows the pile motion to vary from the free-field motion. Moreover, from the observation evidence from the Northridge and Kobe earthquakes, Papazoglou and Elnashai [13] found that many failure modes are mainly caused by vertical earthquake motion. Hence, investigations of the vertical kinematic response of the pile, which is typically induced by the vertical P-wave, are an important research subject.

Over the past few decades, methods have been developed to investigate the vertical kinematic response of the pile. Mamoon and Ahmad [14] investigated the seismic response using the boundary element method. Ji and Pak [15] developed a boundary integral equation method to investigate the dynamic response of a thin-walled pile embedded in isotropic soil subject to a vertical incidence of the P-wave. Later, this work was extended to the study of a pile embedded in a transversely isotropic half-space with the aid of ring-loads

Green's functions [5,16]. Pioneered by the work of Novak and Aboul-Ella [17], Mylonakis and Gazetas [18] developed a rod-on-dynamic Winkler foundation model to investigate the kinematic pile response under a vertical incidence of the P-wave. Based on the pioneering work by Nogami and Novák [19], Anoyatis et al. [20] proposed a continuum elastodynamic solution to investigate the vertical kinematic pile–soil interaction. Then, this method was extended to investigate the kinematic response of piles considering three-dimensional wave scattering [9,21]. Later, the solution of floating piles was proposed [22]. Based on a foundation model proposed by Vlasov and Leontiev [23], Liu et al. [24] and Ke et al. [25] developed a new continuum elastodynamic solution to investigate the vertical kinematic pile–soil interaction.

It is worth noting that the surrounding soil in most of the previous studies was assumed to be homogeneous or layered homogeneous. However, due to the construction disturbance effect, the soils around the pile are squeezed and pushed away, and the soil properties vary gradually within the region adjacent to the pile in the radial direction. The effects of pile driving on soil properties have been investigated for the past 50 years [26–30]. Many of the previous studies (including field measurements of shear-wave velocity, field vane shear tests, and unit weight comparisons) have addressed soil properties obtained before and after pile installation [31,32]. All studies have shown that the soil properties are changed in the radial direction during pile-sinking [27]. Over the last few decades, the construction effects have been considered in the study of the inertial response of piles. Veletsos and Dotson [33] proposed an analytical model to study the vertical and torsional vibration of piles, which allows the soil properties to change continuously within the disturbed zone in the radial direction. However, these methods can only simulate the case that the soil properties change in a particular form. Using a series of annular homogeneous zones to simulate the disturbed soil with arbitrarily varying material properties in the radial direction, El Naggar [34] investigated the vertical and torsional vibration of composite soil. In this model, the stiffness of each annular zone is calculated separately and joined together with a number of springs in series. However, the vertical wave effect is ignored. Wang et al. [35] proposed a one-dimensional complex stiffness transfer model to investigate the vertical impedance of composite soil. Yang et al. [36] used a three-dimensional axisymmetric model to study the vertical dynamic response of piles in a radially heterogeneous soil layer. Then, this model was extended to study the vertical vibration of a large-diameter pipe pile [37]. However, the construction disturbance effect has only been considered in the study of the inertial response of piles. To date, no study has investigated the kinematic response of piles considering the construction disturbance effect.

The main objective of this paper is to derive a rigorous solution to investigate the kinematic response of end-bearing piles under the excitation of vertical P-waves considering the construction effect. This paper follows the following scheme. First, a generalized mathematical-physical model of this problem is simplified in Section 2. The construction disturbance effect is considered in this study. The disturbed soil adjacent to the pile is modeled by a series of vertical annular homogeneous zones. Based on this assumption, the corresponding governing equations and boundary conditions are presented in Sections 2.2–2.4. Then, the detailed theoretical formulation and the solution of the model are presented in Section 3. In Section 4, the numerical results are delivered through the solution presented in Section 3.

2. Model

2.1. Model Assumptions and Simplification

The model in this problem is depicted in Figure 1. It represents a solid pile embedded in the viscoelastic soil considering the construction disturbance effect. The disturbed soil adjacent to the pile was modeled by N vertical annular homogeneous zones to simulate the construction disturbance effect. The soil in each annular zone was linearly viscoelastic, isotropic, and homogeneous, and the neighboring soil zones were in perfect contact with each other. The outer and inner radii of the jth zone were defined as r_j and r_{j-1}, respectively.

The undisturbed soil was linearly viscoelastic, isotropic, and homogeneous. The pile was elastic with a uniform circular cross-section. The pile length and pile radius were defined as H and r_0, respectively. Both the pile and soil overlaid a rigid bedrock. The excitation of the model was assumed to be a vertically harmonic P-wave, defined as $u_0 e^{i\omega t}$.

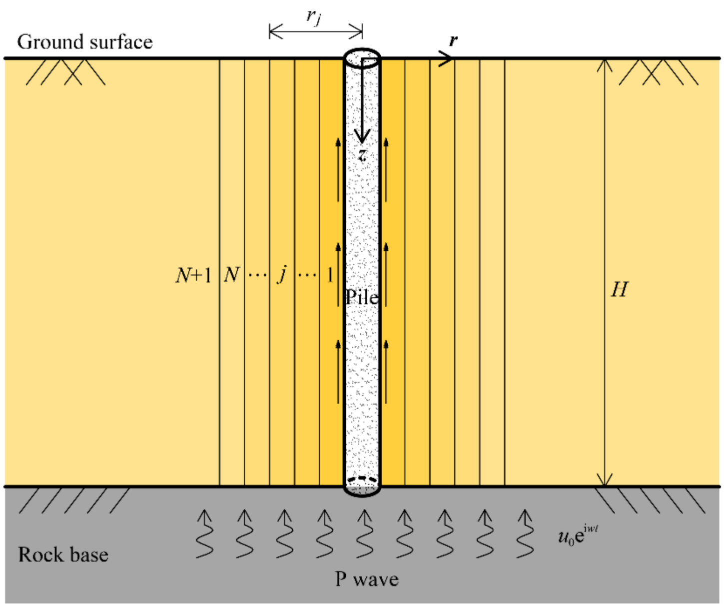

Figure 1. The analytical model of the kinematic response of end-bearing piles under the excitation of vertical P-waves considering the construction effect.

The soil and pile mainly experienced the vertical motion under the excitation of vertically incident harmonic P-waves. The radial displacement was negligible compared with the vertical displacement. For this reason, the radial displacement of the pile was neglected.

2.2. Dynamic Equations of Soil

The displacements of the jth soil zone are denoted as $u_{z,j}(r,z)e^{i\omega t}$. Then, the dynamic equilibrium equation of each soil zone can be expressed as follows [19,20]:

$$\left(\lambda_j^* + 2G_j^*\right)\frac{\partial^2}{\partial z^2}u_{z,j}(r,z) + G_j^*\left(\frac{\partial}{r\partial r} + \frac{\partial^2}{\partial r^2}\right)u_{z,j}(r,z) + \rho_{s,j}\omega^2 u_{z,j}(r,z) = 0 \tag{1}$$

where $G_j^* = G_j(1 + 2i\beta_j)$ and $\lambda_j^* = 2G_j^* v_{s,j}\left(1 - 2v_{s,j}\right)$ are the Lamé constants of the jth soil zone, β_j is the hysteretic damping ratio, and $\rho_{s,j}$ and $v_{s,j}$ are the soil density and Poisson's ratio of the jth soil zone, respectively.

2.3. Dynamic Equation of Pile

Assuming that the harmonic displacement of the pile is $w(z)e^{i\omega t}$, the dynamic equation of the pile can be expressed as follows [19,20]:

$$E_p A\frac{\partial^2 w(z)}{\partial z^2} + f(z) = -\rho_p A\omega^2 w(z) \tag{2}$$

where $E_p = \rho_p V_p^2$ is the Young's modulus of the pile, $A = \pi r_0^2$, r_0 is the radius of the pile, ρ_p is the pile density, V_p is the longitudinal wave velocity of the pile, and $f(z)e^{i\omega t}$ is the frictional force acting on the surface of the pile.

2.4. Boundary Conditions

In addition to the governing equation, the soil and pile displacements should also satisfy the following boundary conditions:

1. The continuity conditions between the adjacent soil zones:

$$\begin{cases} u_{z,j}(r,z)\big|_{r=r_j} = u_{z,j+1}(r,z)\big|_{r=r_j} \\ \tau_{zr,j}(r,z)\big|_{r=r_j} = \tau_{zr,j+1}(r,z)\big|_{r=r_j} \end{cases}, \; j = 1,2,\ldots,N+1 \tag{3}$$

2. The displacements are u_0 at the bottom of the soil layers and pile:

$$u_{z,j}(r,z)\big|_{z=H} = u_0, \; j = 1,2,\ldots,N+1 \tag{4}$$

$$w(z)|_{z=H} = u_0 \tag{5}$$

3. The normal stresses are zero at the ground surface:

$$\sigma_{z,j}(r,z)\big|_{z=0} = 0, j = 1,2,\ldots,N+1 \tag{6}$$

$$\left.\frac{\partial w_p(z)}{\partial z}\right|_{z=0} = 0 \tag{7}$$

4. The displacement converges to free-field at infinite:

$$u_{z,N+1}(r,z)|_{r\to\infty} = u^f_{N+1}(r,z) \tag{8}$$

5. The continuity conditions between the soil and pile:

$$2\pi r_0 \tau_{zr,1}(r_0,z) = f(z) \tag{9}$$

$$u_{z,1}(r_0,z) = w(z) \tag{10}$$

At this point, the mathematical model of the problem has been built as shown above.

3. Theoretical Formulation

Due to the existence of the pile, scattered P and S waves will be generated. The soil motion can be expressed as the sum of the free-field displacement and the scattered soil displacement, expressed as:

$$u_{z,j}(r,z) = u^f_j(z) + u^s_{z,j}(r,z) \tag{11}$$

The free-field displacement is the soil displacement of the half-space under the P-wave incidence. It is obtained as:

$$u^f_{z,j}(z) = \frac{cos\kappa_j z}{cos\kappa_j H}u_0 \tag{12}$$

where $\kappa_j = \sqrt{\rho_{s,j}\omega^2/\left(\lambda_j{}^* + 2G_j{}^*\right)}$.

Using the separation of variables method, the scattered soil displacement can be obtained through Equation (1):

$$u^s_{z,j}(r,z) = \sum_{n=1}^{\infty}\left[A_{j,n}K_0\left(\eta_{j,n}r\right) + B_{j,n}I_0\left(\eta_{j,n}r\right)\right]cos(\beta_n z), \; j = 1,2,\ldots,N+1 \tag{13}$$

Substituting Equations (11)–(13) into Equations (3) and (8), one can obtain:

$$\boldsymbol{M}_{j-1,n}\left(r_{j-1}\right)\begin{bmatrix} A_{j-1,n} \\ B_{j-1,n} \end{bmatrix} = \boldsymbol{M}_{j,n}\left(r_{j-1}\right)\begin{bmatrix} A_{j,n} \\ B_{j,n} \end{bmatrix} + \boldsymbol{a}_{j,n} \tag{14}$$

$$B_{N+1,n} = 0 \tag{15}$$

where $\boldsymbol{M}_{j,n}(r)$ and $\boldsymbol{a}_{j,n}$ are presented in in Appendix A.

Then, the following relation between $\begin{bmatrix} A_{1,n} \\ B_{1,n} \end{bmatrix}$ and $\begin{bmatrix} A_{N+1,n} \\ B_{N+1,n} \end{bmatrix}$ can be obtained:

$$\begin{bmatrix} A_{1,n} \\ B_{1,n} \end{bmatrix} = \boldsymbol{Q}_n \begin{bmatrix} A_{N+1,n} \\ B_{N+1,n} \end{bmatrix} + \boldsymbol{R}_n \tag{16}$$

where

$$\boldsymbol{Q}_n = \prod_{j=1}^{N} \boldsymbol{M}_{j,n}^{-1}(r_j)\boldsymbol{M}_{j+1,n}(r_j) \tag{17}$$

$$\boldsymbol{R}_n = \sum_{j=2}^{N}\prod_{k=1}^{j-1} \boldsymbol{M}_{k,n}^{-1}(r_k)\boldsymbol{M}_{k+1,n}(r_k)\boldsymbol{M}_{j,n}^{-1}(r_j)\boldsymbol{a}_{j+1,n} + \boldsymbol{M}_{1,n}^{-1}(r_1)\boldsymbol{a}_{2,n} \tag{18}$$

The frictional force acting on the surface of the pile can be derived through Equation (9), written as:

$$f(z) = 2\pi r_0 \tau_{zr}(r_0, z) = 2\pi r_0 \sum_{n=1}^{\infty} \begin{bmatrix} M_{1,n}^{21}(r_0) & M_{1,n}^{22}(r_0) \end{bmatrix} \begin{bmatrix} A_{1,n} \\ B_{1,n} \end{bmatrix} cos(\beta_{1,n} z) \tag{19}$$

Substituting Equation (19) into Equation (2), the pile displacement is obtained as:

$$\begin{aligned} w_p(z) &= a_p sin(\chi_p z) + b_p cos(\chi_p z) \\ &\quad - \frac{2\sum_{n=1}^{\infty} \begin{bmatrix} M_{1,n}^{21}(r_0) & M_{1,n}^{22}(r_0) \end{bmatrix} \begin{bmatrix} A_{1,n} \\ B_{1,n} \end{bmatrix}}{(\rho_p \omega^2 - E_p \beta_n^2) r_0} cos(\beta_n z) \end{aligned} \tag{20}$$

where $\chi_p = \omega / \sqrt{E_p/\rho_p}$

Substituting Equation (20) into Equations (5) and (7), one can obtain:

$$a_p = 0 \tag{21}$$

$$b_p = \frac{u_0}{cos(\chi_p H)} \tag{22}$$

Substituting Equations (11), (16) and (20) into Equation (10), one can obtain:

$$\begin{aligned} &\begin{bmatrix} M_{1,n}^{11}(r_0) + \frac{2M_{1,n}^{21}(r_0)}{(\rho_p\omega^2 - E_p\beta_n^2)r_0} & M_{1,n}^{12}(r_0) + \frac{2M_{1,n}^{22}(r_0)}{(\rho_p\omega^2 - E_p\beta_n^2)r_0} \end{bmatrix} \boldsymbol{Q}_n \begin{bmatrix} A_{N+1,n} \\ B_{N+1,n} \end{bmatrix} \\ &= \frac{2a_p}{H}\int_0^H sin(\chi_p z)cos(\beta_n z)dz + \frac{2b_p}{H}\int_0^H cos(\chi_p z)cos(\beta_n z)dz \\ &- \frac{2u_0}{H}\int_0^H \frac{cos(\chi_{1,n} z)}{cos\chi_{1,n} H} cos(\beta_n z)dz \\ &- \begin{bmatrix} M_{1,n}^{11}(r_0) + \frac{2M_{1,n}^{21}(r_0)}{(\rho_p\omega^2 - E_p\beta_n^2)r_0} & M_{1,n}^{12}(r_0) + \frac{2M_{1,n}^{22}(r_0)}{(\rho_p\omega^2 - E_p\beta_n^2)r_0} \end{bmatrix} \boldsymbol{R}_n \end{aligned} \tag{23}$$

Then, the unknown coefficient $A_{N+1,n}$ can be obtained through the above equation. With $A_{N+1,n}$ and $B_{N+1,n}$ obtained, the pile displacement can be determined. The numerical results in Section 4 are delivered through Equation (23) by MATLAB programming.

The kinematic response factor is defined as:

$$I_u = \frac{w_p(0)}{u_{N+1}^f(0)} \tag{24}$$

The kinematic amplification factor is defined as:

$$A = \frac{w_p(0)}{u_0} \tag{25}$$

4. Numerical Results and Discussions

4.1. Verification and Comparisons

The disturbed soil adjacent to the pile was modeled by N vertical annular homogeneous zones. To accurately model the gradually varied soil properties, the number of the divided annular zone should be large enough, and the proposed solution should be converged with the increase in N. Figure 2 shows the effect of N on the pile response. η is the disturbance degree, defined as $\eta = G_1/G_{N+1}$. η = 1 represents the case where the soil is undisturbed. η > 1 represents the case where surrounding the soil is strengthened. η < 1 represents the case where the surrounding soil is weakened. The available parameters used here are shown in Table 1. It can be seen from Figure 2 that the kinematic response factors eventually approach a certain value for a specific case after N = 15. That means the results converged and sufficient accuracy guaranteed for $N \geq 15$.

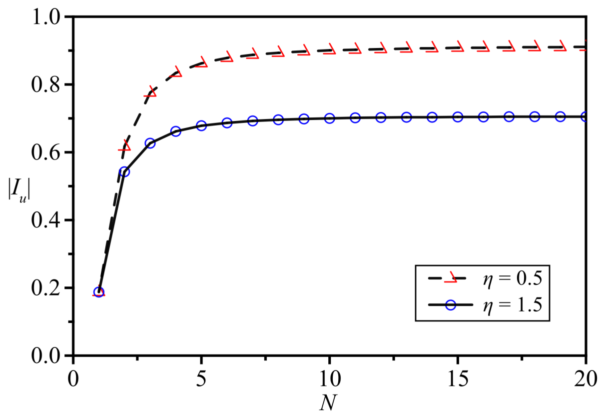

Figure 2. The effect of N on the kinematic response of piles.

Table 1. Available parameters used in the paper.

Pile				Surrounding Soil				
r_0 (m)	H (m)	ρ_p (kg/m^3)	E_p (GPa)	$\rho_{s,j}$ (kg/m^3)	β_j	$v_{s,j}$	G_{N+1} (MPa)	Δr (m)
0.5	20	2500	36	1800	0.02	0.4	36	0.2

The proposed solution can be degenerated to the general case that the pile is embedded in the undisturbed soil, as in Dai et al. [9]. Figure 3 compares the kinematic response of the piles from the present solution by letting η = 1 and that of Winkler model [18], a finite element model [20], an elastodynamic continuum model [20], and a three-dimensional model [9]. The available parameters used here are the same as that adopted in Dai et al. [9]. The dimensional frequency is defined as $\omega = \frac{2H\omega}{\pi V_p}$, where V_p is the wave velocity of the P wave. From the above comparation, the degenerated solution is in good agreement with that of Dai et al. [9]. Since Dai's solution was believed to be rigorous, the presented solution was verified to be reliable. Even though there were divergences between the results of different methods, all appropriate methods can predict the kinematic response of piles approximately.

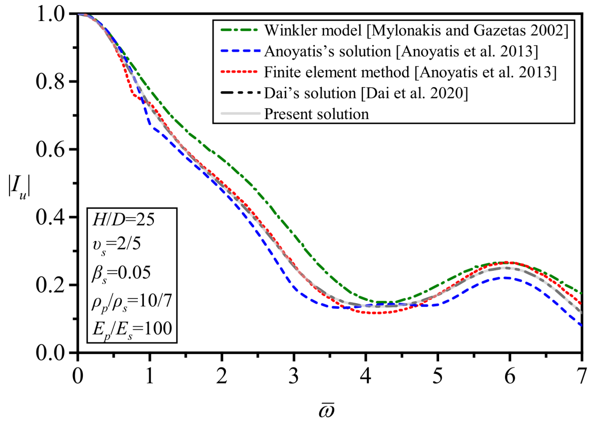

Figure 3. Comparisons of the kinematic response factor between the present solution and that of Mylonakis and Gazetas [18], Anoyatis et al. [20] and Dai et al. [9].

4.2. Discussion

In this section, the effects of disturbance degree (η), disturbance range ($\Delta r = r_N - r_0$), and the length of the pile (H) on the dynamic responses of piles are investigated.

Figure 4 shows the influence of the disturbance degree η on the kinematic response and amplification factors of piles. The kinematic response factor was generally smaller than 1. That means the pile response was generally smaller than the soil response. Moreover, it can be seen that the maximum kinematic response factor was several times larger than minimum kinematic response factor. That means the kinematic factor is mainly dependent on incident frequency. From Figure 4a, the kinematic response factor was generally smaller for the strengthened case ($\eta > 1$) than for the homogeneous one. On the contrary, the kinematic response factor was generally larger for the weakened case ($\eta < 1$) than for the homogeneous one. Obvious resonance can be seen in Figure 4b. There was a significant amplification effect around the resonance frequencies and the resonance frequencies were almost unchanged for different disturbance degrees. Moreover, the strengthened case led to a larger amplification factor than the homogeneous one at the first resonance frequency. On the contrary, the weakened case led to a smaller amplification factor than the homogeneous one at the first resonance frequency. In the high frequency domain, the amplification factor tended to be stable and the pile embedded in the weakened soil led to a larger amplification factor. This was due to the seismic response, which was amplificated for softer soil. The results indicate the resistant earthquake properties of piles increase with the increase in the stiffness of the adjacent soil.

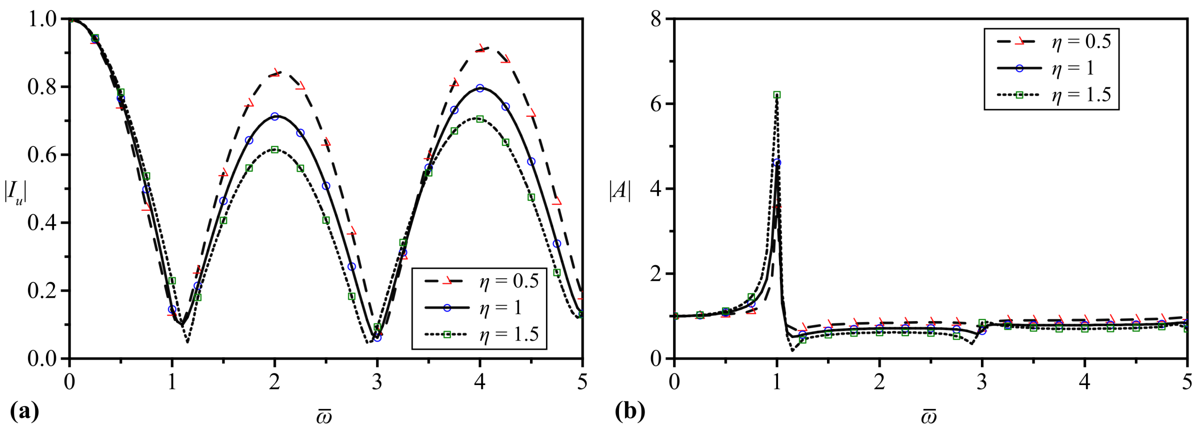

Figure 4. The effects ofs the disturbance degree (η) on the kinematic response and amplification factors of piles (ρ_p = 2500 kg/m^3, E_p = 36 GPa, r_0 = 0.5, v_j = 0.4, β_j = 0.2, G_{N+1} = 36 MPa, H = 20 m, $\triangle r$ = 0.2 m). (**a**) Kinematic response factor; (**b**) Amplification factor.

Figure 5 shows the influence of the disturbance range $\triangle r$ on the kinematic response factor of piles. Figure 5a represents the case of η = 0.5, and Figure 5b represents the case of η = 1.5. Similarly, the kinematic response factor was generally smaller than 1. It is noted that there was nearly no influence of the disturbance range on the dynamic response of piles. This could be due to only a small region of soil around pile being affected during pile-sinking. Compared with the disturbance range, the disturbance degree plays a dominant role in kinematic response of piles. Comparing Figure 5a with 5b, the kinematic response factor was generally larger for the weakened soil case than in the strengthened case.

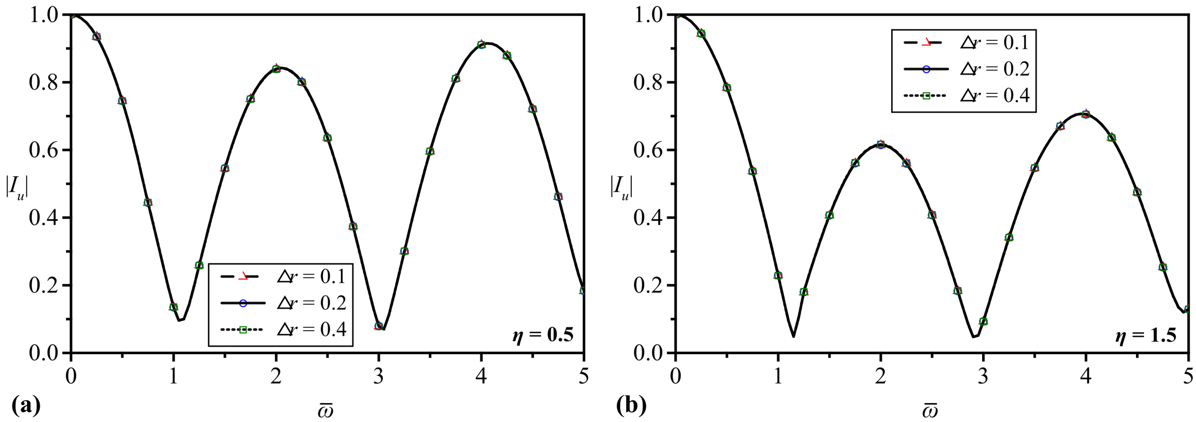

Figure 5. The effects of the disturbance range ($\triangle r$) on the kinematic response and amplification factors of piles (ρ_p = 2500 kg/m^3, E_p = 36 GPa, r_0 = 0.5, υ_j = 0.4, β_j = 0.2, G_{N+1} = 36 MPa, H = 20 m). (**a**) Kinematic response factor; (**b**) Amplification factor.

Figures 6 and 7 show the influence of pile length H on the kinematic response and amplification factors of piles. Figure 6 represents the case of η = 0.5, and Figure 7 represents the case of η = 1.5. As shown, the kinematic factors fluctuated as the frequency increase. It can be concluded from Figure 6a that the kinematic response factor was generally smaller for larger pile length, overall. On the contrary, the amplification factor at the first resonance frequency was generally larger for larger pile length, overall. In the high frequency domain, short piles generally suffer a larger amplification factor. It is obvious that the normalized resonance frequencies were almost unchanged for different pile length. Since the normalized frequency was the function of the pile length, the real resonance frequencies were different for different pile length. The same conclusions can also be drawn from Figure 7. The results indicate that the earthquake-resistant properties of longer piles are superior to those of structures composed of shorter piles.

Figure 8 shows the effects of disturbance degree (η) on the soil displacements. Figure 8a represents the case of η = 0.5, Figure 8b represents the case of η = 1, and Figure 8c represents the case of η = 1.5. As shown, the soil displacements on the ground was suppressed in a specified region adjacent to the pile. The region of influence is about six times the pile's radius. The influence of soil disturbance on soil displacements was much less. Despite this, it can be concluded from the comparison that the soil displacement was slightly smaller for the strengthened soil than for the weakened soil. Moreover, the region of influence for weakened soil was slightly larger for the weakened soil than for the strengthened soil. The law of the soil response was consistent with that of the pile response. This was due to the seismic response, which was amplificated for softer soil.

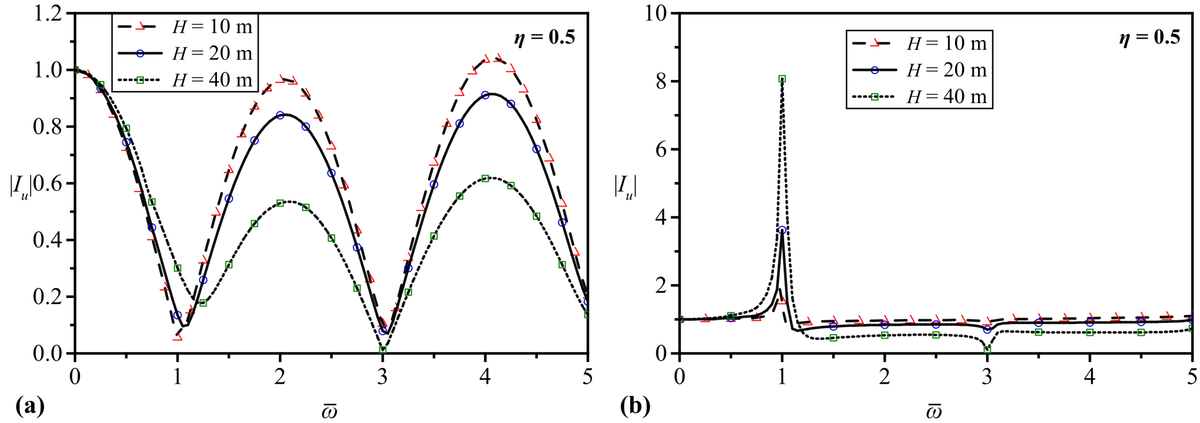

Figure 6. The effects of the pile length (H) on the kinematic response and amplification factors of piles (ρ_p = 2500 kg/m^3, E_p = 36 GPa, r_0 = 0.5, v_j = 0.4, β_j = 0.2, G_{N+1} = 36 MPa, H = 20 m, η = 0.5). (**a**) Kinematic response factor; (**b**) Amplification factor.

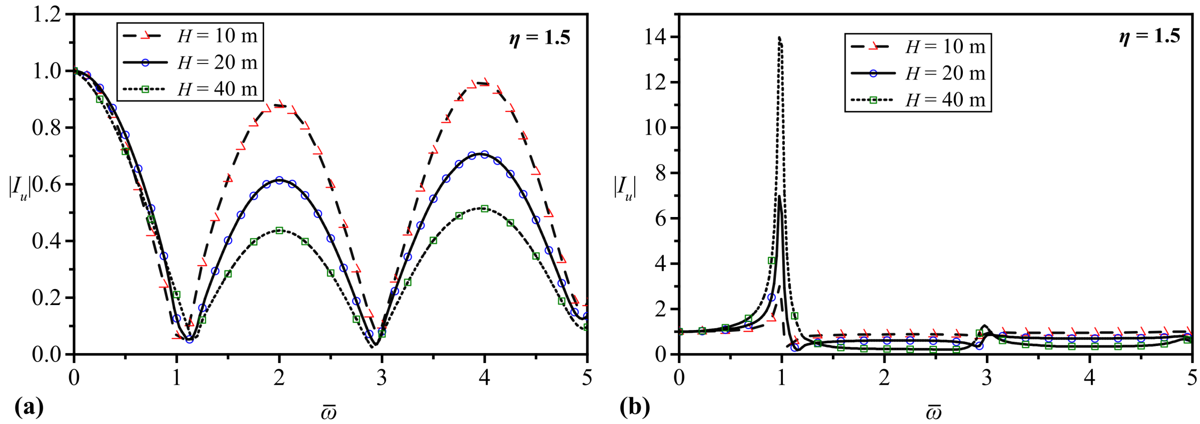

Figure 7. The effects of the pile length (H) on the kinematic response and amplification factors of piles (ρ_p = 2500 kg/m^3, E_p = 36 GPa, r_0 = 0.5, v_j = 0.4, β_j = 0.2, G_{N+1} = 36 MPa, H = 20 m, η = 1.5). (**a**) Kinematic response factor; (**b**) Amplification factor.

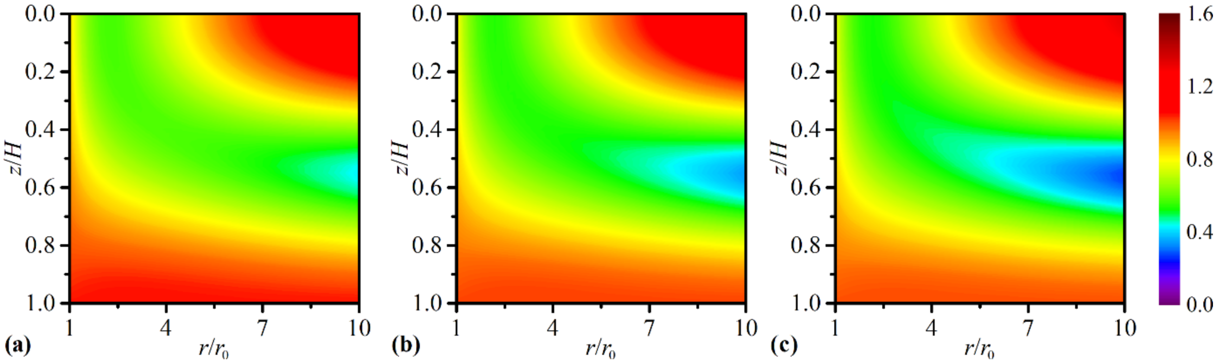

Figure 8. The effects of the disturbance degree (η) on the soil displacements (ρ_p = 2500 kg/m^3, E_p = 36 GPa, r_0 = 0.5, v_j = 0.4, β_j = 0.2, G_{N+1} = 36 MPa, H = 20 m). (**a**) η = 0.5; (**b**) η = 1; (**c**) η = 1.5.

5. Conclusions

An elastodynamic continuum model to investigate the kinematic response of end-bearing piles under the excitation of vertical P-waves was proposed in this paper. This solution is rigorous in theory and considers the actual situation during the installation of the pile. To address the soil properties changed in the radial direction during pile-sinking, the disturbed soil adjacent to the pile was modeled by a series of vertical annular homogeneous zones. Based on this assumption, the detailed formulation and solution of the model was conducted. The obtained solution was verified by comparison with the existing degenerated case.

The parametric studies show that the construction effect has a significant influence on the kinematic response of piles:

(1) From the investigation of the effect of disturbance degree, it was found that the resistant earthquake properties of piles increased if the surrounding soil was strengthened during the process of construction. On the contrary, the resistant earthquake properties of piles decreased if the surrounding soil was weakened during pile-sinking.
(2) Through the investigation of the effect of the disturbance range, it was found that there was nearly no influence of the disturbance range on the dynamic response of piles.
(3) It was found that the construction effect mainly affected a specific region around the pile. The soil response was slightly smaller for the strengthened soil than for the weakened soil.
(4) The earthquake-resistant properties of longer piles were superior to those of structures composed of shorter piles.

Author Contributions: Conceptualization, D.D., Y.Z. (Yunfei Zhang) and Z.L.; methodology, D.D., Y.Z. (Yanjie Zhang) and Z.L.; software, D.D., Y.Z. (Yunfei Zhang) and Z.W.; validation, D.D., Y.Z. (Yanjie Zhang), Z.W. and Z.L.; formal analysis, D.D., Z.W., Y.Z. (Yanjie Zhang) and Y.Z. (Yunfei Zhang); investigation, Y.Z. (Yanjie Zhang) and Z.L.; resources, D.D.; data curation, D.D.; writing—original draft preparation, D.D.; writing—review and editing, Z.W. and Z.L.; visualization, Z.W.; supervision, D.D. and Z.L.; project administration, D.D., Y.Z. (Yanjie Zhang) and Z.L.; funding acquisition, D.D. and Y.Z. (Yanjie Zhang). All authors have read and agreed to the published version of the manuscript.

Funding: This research was funded by the key science and technology special program of Yunnan province, grant number 202102AF080001; the Fundamental Research Funds for the Central Universities, grant number B210202042; the National Natural Science Foundation of China, grant number 52108314; and the China Postdoctoral Science Foundation funded project, grant number 2020M681475.

Institutional Review Board Statement: Not applicable.

Informed Consent Statement: Not applicable.

Data Availability Statement: The data presented in this study are available on request from the corresponding author.

Conflicts of Interest: The authors declare no conflict of interest. The funders had no role in the design of the study; in the collection, analyses, or interpretation of data; in the writing of the manuscript; or in the decision to publish the results.

Appendix A

$$\boldsymbol{M}_{j,n}(r) = \begin{bmatrix} M_{j,n}^{11}(r) & M_{j,n}^{12}(r) \\ M_{j,n}^{21}(r) & M_{j,n}^{22}(r) \end{bmatrix}, \ j = 1,2,\ldots,N+1 \tag{A1}$$

$$M_{j,n}^{11}(r) = K_0(\eta_{j,n}r) \tag{A2}$$

$$M_{j,n}^{12}(r) = I_0(\eta_{j,n}r) \tag{A3}$$

$$M_{j,n}^{21}(r) = -G'_j\eta_{j,n}K_1(\eta_{j,n}r) \tag{A4}$$

$$M_{j,n}^{22}(r) = G'_j\eta_{j,n}I_1(\eta_{j,n}r) \tag{A5}$$

$$a_{j,n} = \begin{bmatrix} \int_0^H \frac{2}{H}\left[\frac{u_0 cos\left(\chi_{j,s}z\right)}{cos\chi_{j,s}H} - \frac{u_0 cos\left(\chi_{j-1,s}z\right)}{cos\chi_{j-1,s}H}\right] cos(\beta_n z)dz \\ 0 \end{bmatrix} \tag{A6}$$

References

1. Zhao, Z.H.; Kouretzis, G.; Sloan, S.W.; Gao, Y.F. Effect of geometric nonlinearity on the ultimate lateral resistance of piles in clay. *Comput. Geotech.* **2018**, *105*, 110–115. [CrossRef]
2. Dai, D.H.; El Naggar, M.H.; Zhang, N.; Gao, Y.F.; Li, Z.Y. Vertical vibration of a pile embedded in radially disturbed viscoelastic soil considering the three-dimensional nature of soil. *Comput. Geotech.* **2019**, *111*, 172–180. [CrossRef]
3. Wu, J.T.; Wang, K.H.; El Naggar, M.H. Dynamic response of a defect pile in layered soil subjected to longitudinal vibration in parallel seismic integrity testing. *Soil Dyn. Earthq. Eng.* **2019**, *121*, 168–178. [CrossRef]
4. Wu, J.T.; Wang, K.H.; El Naggar, M.H. Half-space dynamic soil model excited by known longitudinal vibration of a defective pile. *Comput. Geotech.* **2019**, *112*, 403–412. [CrossRef]
5. He, R.; Kaynia, A.M.; Zhang, J.S.; Chen, W.Y. Seismic response of monopiles to vertical excitation in offshore engineering. *Ocean Eng.* **2020**, *216*, 108120. [CrossRef]
6. Meng, K.; Cui, C.Y.; Liang, Z.M.; Li, H.J.; Pei, H.F. A new approach for longitudinal vibration of a large-diameter floating pipe pile in visco-elastic soil considering the three-dimensional wave effects. *Comput. Geotech.* **2020**, *128*, 103840. [CrossRef]
7. Cui, C.Y.; Meng, K.; Xu, C.S.; Liang, Z.M.; Li, H.J.; Pei, H.F. Analytical solution for longitudinal vibration of a floating pile in saturated porous media based on a fictitious saturated soil pile model. *Comput. Geotech.* **2021**, *131*, 103942. [CrossRef]
8. Zhang, S.P.; Zhang, J.H.; Ma, Y.B.; Pak, R.Y.S. Vertical dynamic interactions of poroelastic soils and embedded piles considering the effects of pile-soil radial deformations. *Soils Found.* **2021**, *61*, 16–34. [CrossRef]
9. Dai, D.H.; El Naggar, M.H.; Zhang, N.; Gao, Y.F. Kinematic response of an end-bearing pile subjected to vertical P-wave considering the three-dimensional wave scattering. *Comput. Geotech.* **2020**, *120*, 103368. [CrossRef]
10. Dai, D.H.; El Naggar, M.H.; Zhang, N.; Wang, Z.B. Rigorous solution for kinematic response of floating piles to vertically propagating S-waves. *Comput. Geotech.* **2021**, *137*, 104270. [CrossRef]
11. Kim, J.; Yun, S.K.; Kang, M.; Kang, G. Behavior Characteristics of Single Batter Pile under Vertical Load. *Appl. Sci.* **2021**, *11*, 4432. [CrossRef]
12. Ma, J.; Han, S.; Gao, X.; Li, D.; Guo, Y.; Liu, Q. Dynamic Lateral Response of the Partially-Embedded Single Piles in Layered Soil. *Appl. Sci.* **2022**, *12*, 1504. [CrossRef]
13. Papazoglou, A.J.; Elnashai, A.S. Analytical and field evidence of the damaging effect of vertical earthquake ground motion. *Earthq. Eng. Struct. Dyn.* **1996**, *25*, 1109–1137. [CrossRef]
14. Mamoon, S.M.; Ahmad, S. Seismic response of piles to obliquely incident SH, SV, and P waves. *J. Geotech. Eng.* **1990**, *116*, 186–204. [CrossRef]
15. Ji, F.; Pak, R.Y.S. Scattering of vertically-incident P-waves by an embedded pile. *Soil Dyn. Earthq. Eng.* **1996**, *15*, 211–222. [CrossRef]
16. Shahmohamadi, M.; Khojasteh, A.; Rahimian, M.; Pak, R.Y.S. Seismic response of an embedded pile in a transversely isotropic half-space under incident P-wave excitations. *Soil Dyn. Earthq. Eng.* **2011**, *31*, 361–371. [CrossRef]
17. Novak, M.; Aboul-Ella, F. Impedance functions of piles in layered media. *J. Eng. Mech. Div.* **1978**, *104*, 643–661. [CrossRef]
18. Mylonakis, G.; Gazetas, G. Kinematic pile response to vertical P-wave seismic excitation. *J. Geotech. Geoenviron. Eng.* **2002**, *128*, 860–867. [CrossRef]
19. Nogami, T.; Novák, M. Soil-pile interaction in vertical vibration. *Earthq. Eng. Struct. Dyn.* **1976**, *4*, 277–293. [CrossRef]
20. Anoyatis, G.; Di Laora, R.; Mylonakis, G. Axial kinematic response of end-bearing piles to P waves. *Int. J. Numer. Anal. Meth. Geomech.* **2013**, *37*, 2877–2896. [CrossRef]
21. Zheng, C.J.; Kouretzis, G.; Luan, L.B.; Ding, X.M. Kinematic response of pipe piles subjected to vertically propagating seismic P-waves. *Acta Geotech.* **2021**, *16*, 895–909. [CrossRef]
22. Dai, D.; El Naggar, M.H.; Zhang, N.; Wang, Z. Rigorous solution for kinematic response of floating piles subjected to vertical P-wave. *Appl. Math. Model.* **2022**, *106*, 114–125. [CrossRef]
23. Vlasov, V.Z.; Leontiev, U.N. *Beams, Plates and Shells on Elastic Foundations*, 1st ed.; Israel Program for Scientific Translations: Jerusalem, Israel, 1966; pp. 47–89, (Translated from Russian).
24. Liu, Q.J.; Deng, F.J.; He, Y.B. Kinematic response of single piles to vertically incident P-waves. *Earthq. Eng. Struct. Dyn.* **2014**, *43*, 871–887. [CrossRef]
25. Ke, W.H.; Zhang, C.; Deng, P. Kinematic response of single piles to vertical P-waves in multilayered soil. *J. Earthq. Tsunami* **2015**, *9*, 1550004. [CrossRef]
26. Orrje, O.; Broms, B.B. Effects of pile driving on soil properties. *J. Soil Mech. Found. Div.* **1967**, *93*, 59–73. [CrossRef]
27. Flaate, K. Effects of pile driving in clays. *Can. Geotech. J.* **1972**, *9*, 81–88. [CrossRef]
28. Gong, X.N.; Li, X.H. Several mechanical problems in compacting effects of static piling in soft clay ground. *Eng. Mech.* **2000**, *17*, 7–13.

29. Hunt, C.E.; Pestana, J.M.; Bray, J.D.; Riemer, M. Effect of pile driving on static and dynamic properties of soft clay. *J. Geotech. Geoenviron. Eng.* **2002**, *128*, 13–24. [CrossRef]
30. Li, L.; Luo, Y.; Peng, J.; Liao, Z. Theoretical analysis of the influence of drilling compaction on compressional wave velocity in hydrate-bearing sediments. *Energy Sci. Eng.* **2019**, *7*, 420–430. [CrossRef]
31. Holtz, W.G.; Lowitz, C.A. Effects of driving displacement piles in lean clay. *J. Soil Mech. Found. Div.* **1965**, *91*, 1–13. [CrossRef]
32. Bozozuk, M.; Fellenius, B.H.; Samson, L. Soil disturbance from pile driving in sensitive clay. *Can. Geotech. J.* **1978**, *15*, 346–361. [CrossRef]
33. Veletsos, A.S.; Dotson, K.W. Vertical and torsional vibration of foundations in inhomogeneous media. *J. Geotech. Eng.* **1988**, *114*, 1002–1021. [CrossRef]
34. El Naggar, M.H. Vertical and torsional soil reactions for radially inhomogeneous soil layer. *Struct. Eng. Mech.* **2000**, *10*, 299–312. [CrossRef]
35. Wang, K.H.; Yang, D.Y.; Zhang, Z.Q.; Leo, C.J. A new approach for vertical impedance in radially inhomogeneous soil layer. *Int. J. Numer. Anal. Meth. Geomech.* **2012**, *36*, 697–707. [CrossRef]
36. Yang, D.Y.; Wang, K.H.; Zhang, Z.Q.; Leo, C.J. Vertical dynamic response of pile in a radially heterogeneous soil layer. *Int. J. Numer. Anal. Meth. Geomech.* **2009**, *33*, 1039–1054. [CrossRef]
37. Li, Z.Y.; Wang, K.H.; Wu, W.B.; Leo, C.J.; Wang, N. Vertical vibration of a large-diameter pipe pile considering the radial inhomogeneity of soil caused by the construction disturbance effect. *Comput. Geotech.* **2017**, *85*, 90–102. [CrossRef]